Effect of Alloy Composition on Microstructure and Martensitic Transformation Temperature of a Zr-Cu Shape Memory Alloy

Hitoo Tokunaga*
National Institute of Technology, Kagoshima College, 1460-1, Shinkou, Hayato-Cho, Kirishima city, Japan.

* Corresponding author. Tel.: +81-995-42-9100; email: h-tokunaga@kagoshima-ct.ac.jp
Manuscript submitted June 10, 2018; accepted August 8, 2018.
doi: 10.17706/ijmse.2018.6.4.93-98

Abstract: Zr-Cu binary and Zr-Cu-Al ternary alloys with different compositions were fabricated using arc melting. The phase structure and martensitic transformation temperatures of the alloys were investigated using X-ray diffraction and differential scanning calorimetry, respectively. It was found that the ZrCu martensitic phase was formed as an intermetallic compound in the near-equiatomic Zr-Cu binary alloy. On the other hand, both the ZrCu martensitic and parent phases were formed in the Zr-Cu-Al ternary alloy. In addition, it was confirmed that the martensitic transformation temperature of ZrCu decreased with addition of Al to the base alloy. Therefore, it was found that addition of Al to the equiatomic Zr-Cu alloy can effectively control the microstructure and martensitic transformation temperature.

Key words: Shape memory alloy, ZrCu, martensitic transformation, phase structure, alloy composition.

1. Introduction

Residual strain recovery behavior in shape memory alloys (SMAs) can be induced by a reversible martensitic transformation (MT) of specific intermetallic compounds. Previous studies demonstrated that some alloys exhibit shape memory behavior, where the most famous SMA is the Ti-Ni system [1]-[7]. The B2 TiNi(P) system, where P refers to the parent phase, was observed in the near-equiatomic Ti-Ni alloy over 630 °C and showed a MT to B19' TiNi(M), where M refers to the martensitic phase, under fast cooling. In addition, TiNi(M) exhibited a reverse MT to TiNi(P) during heating. The Ti-Ni SMA possesses superior shape memory properties, such as a high strain recovery ability of 8% or more [8]. Furthermore, its shape recovery temperatures can be controlled by alloy composition (atomic ratio of Ti to Ni); both MT and reverse MT temperatures decrease by approximately 100°C with an increase in Ni concentration of only 1 at.%. However, the application of Ti-Ni SMAs is limited to temperatures below 100 °C as the reverse MT temperature of the SMAs cannot be controlled above this temperature [9]. Therefore, fabrication of novel SMA materials operating above 100 °C is necessary for progress in science and technology.

Zr-Cu system alloys have considerable potential as high-temperature SMA materials [10], [11]. The intermetallic compound ZrCu exhibits a similar reversible MT behavior to TiNi, and the reverse MT start and finish temperatures of ZrCu are 250 °C and 300 °C [10], respectively. On the other hand, it has also been reported that it is not possible to control both the MT and reverse MT temperatures of the Zr-Cu binary only by adjusting the alloy composition. Recently, the possibility of controlling the MT temperature of ZrCu using additional elements was demonstrated. However, more detailed studies are necessary to clarify the effect of alloy compositions on the shape memory behavior of Zr-Cu system alloys.

The objective of the present study was to clarify the effect of alloy composition on the phases and MT temperatures of near-equiatomic Zr-Cu system alloys. First, near-equiatomic Zr-Cu binary and ternary alloys with different alloy compositions were fabricated. Then, the effect of alloy composition on the phases of fabricated Zr-Cu system alloys was investigated using X-ray diffraction (XRD). In addition, the MT temperatures of the fabricated Zr-Cu system alloys were investigated using differential scanning calorimetry (DSC). Furthermore, based on DSC methodology, quantitative analysis of the volume fraction of ZrCu in the fabricated alloys was undertaken and the compositional dependence was investigated.

2. Experimental Procedure

2.1. Materials and Specimens

Both Zr-Cu binary and Zr-Cu system ternary alloys with different alloy compositions were fabricated using an arc melting furnace. The nominal alloy compositions and abbreviations of the fabricated alloys are summarized in Table 1. In the case of the Zr-Cu binary alloy, near-equiatomic Zr-Cu binary alloys (Zr45, Zr50, and Zr55) were fabricated, along with two intermetallic compounds, Zr_7Cu_{10} (Zr41) and Zr_2Cu (Zr67). In the case of the ternary alloy, Al was used as the third element to produce a Zr-Cu-Al system.

Table 1. Nominal Alloy Compositions and Abbreviations of Fabricated Alloys

	Nominal alloy composition	Abbreviations
Binary alloy $Zr_x - Cu_{(100-x)}$	Zr_{41}-Cu_{59} (x = 41at.%)	Zr41
	Zr_{45}-Cu_{55} (x = 45 at.%)	Zr45
	Zr_{50}-Cu_{50} (x = 50 at.%)	Zr50
	Zr_{55}-Cu_{45} (x = 55 at.%)	Zr55
	Zr_{67}-Cu_{33} (x = 67 at.%)	Zr67
Ternary alloy $(Zr\text{-}Cu)_{(100-y)/2} - Al_y$	Zr_{47}-Cu_{47}-Al_6 (y = 6 at.%)	6Al

The master alloy ingots were fabricated by arc melting a mixture of pure Zr, Cu, and Al in an Ar atmosphere. The master alloy ingots were remelted several times in order to ensure chemical homogeneity. Fig. 1 (a) shows the geometry (button-type samples) and size of the fabricated master alloy ingot. Plate-type specimens with a thickness of about 2 mm were machined using a cutting machine (Buehler, Isomet LS) and a diamond grindstone (Fig. 1(b)). Furthermore, the disk-type specimen was machined using an electric discharge machine (Fig. 1(c)).

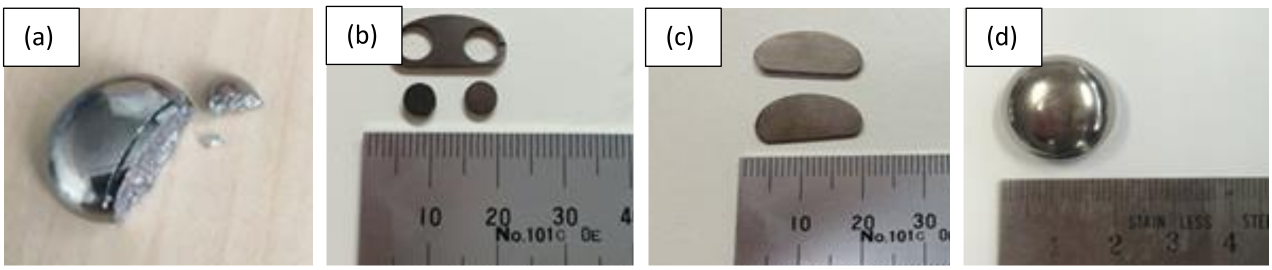

Fig. 1. Fabrication of materials and specimens. (a) master alloy ingot, (b)Plate-type specimen,(c) disk-type specimen, and (d) broken master alloy and fragments of Zr41.

2.2. Phase Structure and Martensitic Transformation Temperature

The microstructure of the plate-type specimens was analyzed at room temperature using an XRD system with CuKα radiation. In addition, DSC was performed under a flow of nitrogen gas. The disk-shaped specimens were heated to 350 °C, then cooled to room temperature (binary alloy) or -150 °C (ternary alloy) with a heating and cooling rate of 0.167 °C/s. It should be noted that, in the present study, evaluation of the Zr41 alloy was not performed as the plate-type specimen of this alloy could not be prepared by the machining process described above; as shown in Fig. 1(d), the Zr41 alloy much more brittle than the other alloys.

3. Results and Discussions

3.1. Compositional Dependence of the Microstructure

The effect of alloy composition on the microstructure of the Zr-Cu system alloys were investigated by XRD. Fig. 2 shows XRD patterns, and it can be seen from the figure that the microstructure of the samples depended on the alloy composition. In particular, the phases of the Zr-Cu binary alloys could be explained in terms of the Zr-Cu equilibrium phase diagram. As shown in Fig. 2 (a)–(c),the dominant phases of the Zr45, Zr50, and Zr55 alloys were ZrCu(M) +Zr_7Cu_{10}, ZrCu(M), and ZrCu(M) + Zr_2Cu, respectively. In addition, the dominant phase the Zr67 alloy was Zr_2Cu (Fig. 2(d)). These results indicate that the MT from ZrCu(P) to ZrCu(M) of occurred during solidification of the Zr45, Zr50, and Zr55 alloys, and a MT finish temperature (M_f) of ZrCu(P) was higher than room temperature. On the other hand, in the case of the Zr-Cu system ternary alloy (6Al), both ZrCu(M) and ZrCu(P) were formed in the alloy, as shown in Fig. 2 (e). This implies that the addition of Al to the Zr-Cu system induced a decrease in the MT start temperature (M_s) and M_f of ZrCu(P). The quantitative experimental M_s and M_f values for ZrCu are discussed in the following section.

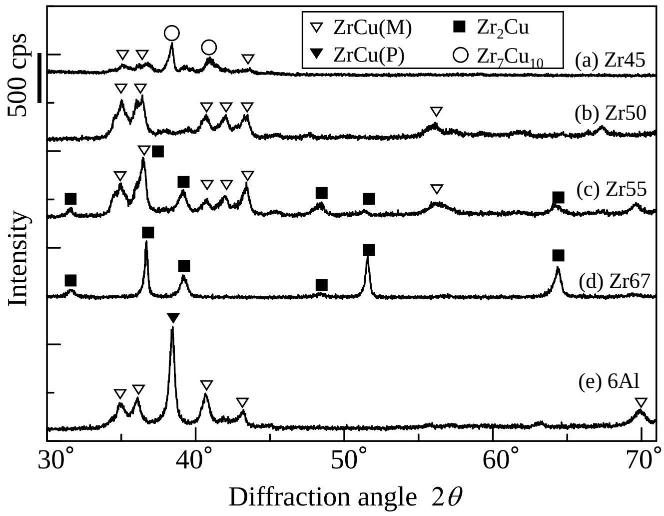

Fig. 2. XRD patterns of fabricated Zr-Cu system alloys.

3.2. Martensitic Transformation Temperatures

The start and finish MT temperatures (M_s, M_f) and reverse MT temperature (A_s, A_f) of the Zr-Cu alloys with different compositions were evaluated using DSC, where Fig. 3 shows a representative DSC curve of the Zr50 sample. As the endothermic and exothermic peaks correspond to the reverse MT and MT, respectively, A_s, A_f, M_s, and M_f were obtained, as summarized in Fig.4. It can be seen that A_s, A_f, M_s, and M_f of the Zr-Cu binary alloys (Zr45, Zr50, and Zr55) varied only slightly with changes in the alloy composition. On the other hand, in the case of 6Al, these values were obviously lower than those of the Zr-Cu binary alloys. These results corresponded well with the XRD data shown in Fig. 2. It was confirmed that the addition of Al to the

Zr-Cu system could effectively control the MT temperature of ZrCu.

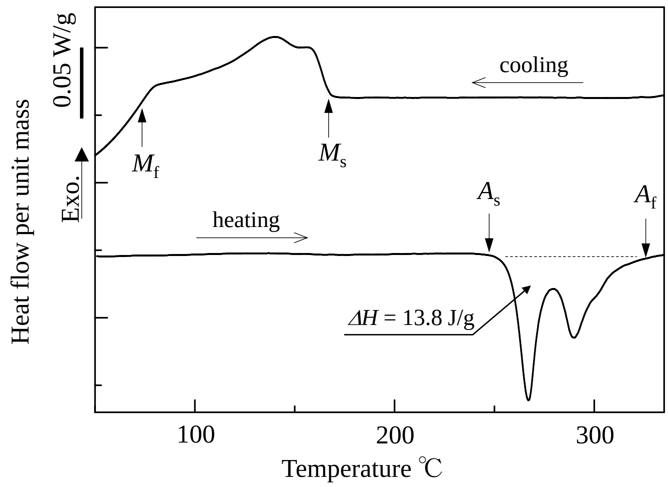

Fig. 3. Endothermic and exothermic reactions of Zr50 alloy obtained by DSC measurement.

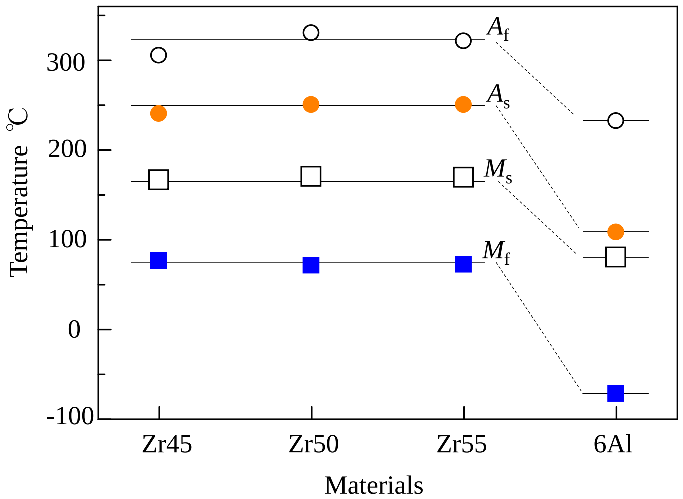

Fig. 4. Martensitic transformation temperatures of Zr45, Zr59 Zr55 and 6Al alloys.

3.3. Volume Fraction of ZrCu

Analysis of the DSC data allowed the volume fraction v_f of a specific crystalline phase to be calculated, corresponding to the ratio of the transformation enthalpy ΔH of a sample to that of a reference material. Here, the volume fraction of ZrCu(M) ($v_{f\ (ZrCu)}$) was estimated from reverse MT enthalpies from DSC data. The relative volume fraction ($v_{f\ (ZrCu)}$) /($v_{f\ (ref)}$) was calculated using the following equation.

$$\frac{v_{f(ZrCu)}}{v_{f\,(ref)}} = \frac{\Delta H_{ZrCu}}{\Delta H_{ref}} \tag{1}$$

where $v_{f\ (ref)}$ is the v_f value of a reference material (here, the Zr50 alloy), and ΔH_{ref} and ΔH_{ZrCu} are the reverse MT enthalpies of the reference material and investigated alloy, respectively. Fig. 5 shows the ($v_{f\ (ZrCu)}$) /($v_{f\ (ref)}$) values of the Zr45, Zr50, Zr55, and 6Al alloys. In the case of the Zr-Cu binary alloys, it was found that the ($v_{f\ (ZrCu)}$) / $v_{f\ (ref)}$) values of the Zr45 and Zr55 alloys were 31% and 80%, respectively. As mentioned in the previous section, the equilibrium phases Zr_7Cu_{10} and/or Zr_2Cu were formed in Zr45 and Zr55. Therefore, the ($v_{f\ (ZrCu)}$) /($v_{f\ (ref)}$) values of the Zr45 and Zr55 alloys were smaller than that of the Zr50 alloy. On the other hand, the ($v_{f\ (ZrCu)}$) /($v_{f\ (ref)}$) value of the 6Al alloy was also 55% of that of the Zr50 alloy, although equilibrium phases were not formed in the 6Al alloy. This suggests that some of the ZrCu in the 6Al alloy did not undergo MT during thermal cycling.

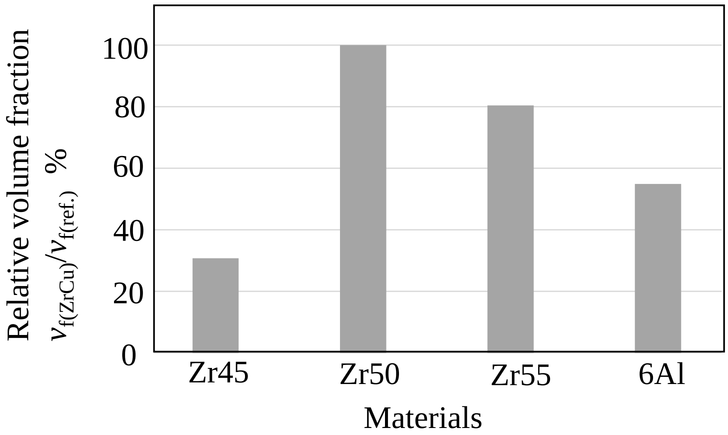

Fig. 5. Estimated relative volume fractions of ZrCu(M) of Zr45, Zr50, Zr55, and 6Al alloys.

4. Conclusion

The effect of alloy composition on the phase structure and MT temperature of Zr-Cu system alloys was investigated and the following results were obtained.

(1) XRD analysis revealed that the Zr47-Cu47-Al6 alloy consisted of ZrCu(M) and ZrCu(P). In addition, it was found that the addition of Al to the Zr-Cu system alloy effectively controlled the MT temperature of ZrCu.

(2) The MT and reverse MT temperatures of the near equiatomic Zr-Cu binary alloys varied only slightly with changes in the alloy composition.

(3) The volume fraction of ZrCu(M) in the Zr47-Cu47-Al6 alloy was only 55% of that in the Zr50–Cu50 alloy.

Acknowledgment

This work was supported by JSPS KAKENHI Grant Number JP16K17987.

References

[1] Gall, K., Tyber, J., Wilkesanders, G., Robertson, O. R., & Hans, J. M. (2008). Effect of microstructure oon the fatigue of hot-rolled and cool-drawn NiTi shape memory alloys. *Materials Science and Engineering A, 486*, 389-403.

[2] Dayananda, G. N., & Subba, R. M. (2008). Effect of strain rate on properties of superelastic NiTi thin wires. *Materials Science and Engineering A, 486*, 96-103.

[3] Tan, L., Dodd, R. A., & Crone, W. C. (2003). Corrosion and wear-corrosion behavior of NiTi modified by plasma source ion implantation. *Biomaterials, 24*, 3931-3939.

[4] Inaba, A., Kimura, K., Iwanaga, H. & Tobushi, H. (1989). A study on mechanical properties of NiTi shape memory alloy (experiments on cyclic characteristics of pseudoelastisity) (in Japanese). *Transactions of the Japan Society of Mechanical Engineers (A), 55(511)*, 628-633.

[5] Ishida, A. (2007). Microstructures and mechanical behaviors of Ti-Ni shape memory thin films formed

by sputtering. *Journal of Japan Institute of Light Metals, 57(7)*, 293-300.

[6] Tang, W., Sundman, B., Sandstrom, R., & Qiu, C. (1999). New modelling of the B2 phase and its associated martensitic transformation in the Ti-Ni system. *Acta Materialia, 47(12)*, 3457-3468.

[7] Frenzel, J., Wieczorek, A., Opahle, I., MaaB, B., Druatz, R., & Eggeler, G. (2015). On the effect of alloy composition on martensite start temperatures and latent heats in Ni-Ti-based shape memory alloys. *Acta Materialia, 90*, 213-231.

[8] Jani, J. M., Leary, M., Subic, A. & Gibson, M. A. (2014). A review of shape memory alloy research, applications and opportunities. *Materials and Design, 56*, 1078-1113.

[9] Firstov, G. S., Van Humbeeck, J., & Koval, Y. N. (2004). High-temperature shape memory alloys Some recent developments. *Materials Science and Engineering A, 378*, 2-10.

[10] Biffi, C. A., Figini, A., & Tuissi, A. (2014). Influence of compositional ratio on microstructure and martensitic transformation of CuZr shape memory alloys. *Intermetallics, 46*, 4-11.

[11] Biffi, C. A, &. TUissi, A. (2014). Hot workability of CuZr-based shape memory alloys for potential high-temperature applications. *Journal of Materials Engineering and Performance, 23(7)*, 2379-2384.

Hitoo Tokunaga was born in Japan, March 8th 1977. He is a Doctor of Engineering, Graduate school of University of Miyazaki, Miyazaki city, Japan, March of 2006.

He is the assistant professor of the National Institute of Technology, Kagoshima College. The college is located in Kirishima city, Kagoshima Prefecture, Japan.

He is the List memberships in professional societies of The Japan Society of Mechanical Engineering, The Society of Materials Science, Japan, The Japan Institute of Metals and Materials, and Association of Shape Memory Alloys.